Multifractal properties of snapshot attractors of random maps

Filipe J. Romeiras
Laboratory for Plasma Research, University of Maryland, College Park, Maryland 20742
and Centro de Electrodinâmica (INIC), Instituto Superior Técnico, 1096 Lisboa Codex, Portugal

Celso Grebogi
Laboratory for Plasma Research, University of Maryland, College Park, Maryland 20742

Edward Ott
Laboratory for Plasma Research, Department of Electrical Engineering and Department of Physics, University of Maryland, College Park, Maryland 20742

(Received 7 August 1989)

We consider qualitative and quantitative properties of "snapshot attractors" of random maps. By a random map we mean that the parameters that occur in the map vary randomly from iteration to iteration according to some probability distribution. By a "snapshot attractor" we mean the measure resulting from many iterations of a *cloud* of initial conditions viewed at a *single* instant (i.e., iteration). In this paper we investigate the multifractal properties of these snapshot attractors. In particular, we use the Lyapunov number partition function method to calculate the spectra of generalized dimensions and of scaling indices for these attractors; special attention is devoted to the numerical implementation of the method and the evaluation of statistical errors due to the finite number of sample orbits. This work was motivated by problems in the convection of particles by chaotic fluid flows.

I. INTRODUCTION

The problem of the effect of random (or "noisy") dynamics on strange attractors can be addressed in two very different ways.

Problem 1. Consider a cloud of initial conditions and evolve it forward in time under a given realization of the noisy dynamics. Then view the resulting measure at a *single instant* of time $t=t_f$, where t_f is large.

Problem 2. Look at the evolution of a *single initial condition* under a realization of the random dynamics, and plot its position in phase space for times t in the range $t_0<t<t_f$, where t_0 and t_f-t_0 are large.

Throughout the present paper, the random dynamical systems we study are maps of the general form

$$\mathbf{x}_{i+1}=\mathbf{F}(\mathbf{x}_i,\mathbf{p}_i)\ , \tag{1}$$

where $\mathbf{x}_i$ and $\mathbf{F}$ are two-dimensional vectors and $\mathbf{p}_i$ is a parameter vector which varies randomly from iteration to iteration, and we take the $\mathbf{p}_i$ to be independent identically distributed random vectors.

In the *absence* of randomness in the dynamical system [e.g., $\mathbf{p}_i=\bar{\mathbf{p}}$ in (1), where $\bar{\mathbf{p}}$ is a fixed parameter], problems 1 and 2 are thought to be typically equivalent for mixing strange attractors. That is, the same measure is generated in the limits

$$t_f\to+\infty$$

for problem 1, and

$$t_0, t_f-t_0\to+\infty$$

for problem 2. In fact, this is rigorously true for hyperbolic attractors as shown by the proof of the existence of a natural measure for such cases.[1] For nonhyperbolic systems, such as the Hénon map, a natural measure is still widely thought to exist. Indeed, numerically, one finds that the procedures specified by problem 1 and by problem 2 yield the same picture of the Hénon attractor and its measure.

The situation is very different, however, when a random dynamical system is considered. The result of the procedure specified in problem 2 is an attractor with a smooth density of points: essentially a *fuzzy* version of the strange attractor that exists in the absence of randomness, where the extent of the fuzziness increases with the amount of the randomness in the system. In contrast, the result of the procedure specified in problem 1 is typically a *fractal* measure. We call this fractal measure a *snapshot attractor.* Note that gross features of a snapshot attractor (e.g., its overall macroscopic shape and position) depend on the time t_f at which it is viewed. Its multifractal properties (i.e., its dimension spectrum) should, however, typically be independent of t_f. While problem 2 has been much studied,[2] problem 1 and its resulting snapshot attractors have received little attention.[3]

Nevertheless, as we shall argue below, problem 1 is very interesting from a number of points of view, and this paper will be devoted to its study. In particular, we present the first investigations of the spectrum of dimensions for the multifractal measure of snapshot attractors of random maps.

 ©1990 The American Physical Society

As motivation for this study, consider the motion of a cloud of particles in an incompressible fluid flow, $\mathbf{v}(\mathbf{x},t)$. If the particles have a density different from that of the fluid and are of not too small a size, they will, in general, move with a velocity which can depart significantly from that of the fluid. That is, the velocity of a particle at $\mathbf{x}$ [denoted $\mathbf{u}(\mathbf{x},t)$] will not be the same as the fluid velocity $\mathbf{v}(\mathbf{x},t)\neq\mathbf{u}(\mathbf{x},t)$. In particular, this is because of the effects of buoyancy, Stokes's drag, inertia, etc.[4] The equations describing the particle trajectories are not volume preserving [in contrast to the case of small particles, where $d\mathbf{x}/dt=\mathbf{v}(\mathbf{x},t)$ and $\nabla\cdot\mathbf{v}=0$]. Thus strange attractors are possible in this case. In particular, for nonrandom temporally steady or periodic flows, it has been shown that the distribution of particles can be on a strange attractor in phase space, and, moreover, the distribution in physical position space can also be fractal.[5] Since the fluid flow $\mathbf{v}(\mathbf{x},t)$ may have chaotic time dependence, however, one is also led to the consideration of particle trajectories in a system which is effectively random. Equation (1) where $\mathbf{F}$ is area contracting may be thought of as the simplest nontrivial (but crude) model of such a situation. In particular, since (1) can yield fractals for problem 1, we expect a "snapshot" of the convected particles in a temporally chaotic fluid flow to also typically reveal a fractal distribution. The related problem of the fractal distribution of the magnitude of the *gradient* of a passive scalar which is convected with the flow ($\mathbf{u}=\mathbf{v}$) has been considered in Refs. 6 and 7. In addition, the fractal distribution of a vector field convected with a fluid flow arises in considerations of the kinematic dynamo problem.[7] In regard to the latter two problems, Ott and Antonsen[6,7] consider a simple two-dimensional baker's map with random parameters as a crude model of the effect of random fluid flow. We also note a similarity between problem 1 and the (much harder) problem of turbulence in fluids. In particular, in the large Reynolds number limit, a snapshot of a fluid that is in a fully developed turbulent state will yield a distribution of vorticity squared which is concentrated on a fractal.[8,9] [Note that, as in problem 1, it is important that a snapshot be taken. If the distribution is averaged over time, as in problem 2, it is smeared out, and the fractal nature is gone (the distribution is a smooth density).] The above discussion is meant to motivate considerations of problem 1, and to make the point that (at least in some general way) such considerations can shed light on situations of physical interest. Undoubtedly other examples, in addition to the above, also exist.

The plan of this paper is as follows. In Sec. II we introduce the snapshot technique which is then used to display the gross qualitative features of attractors of the Hénon and Ikeda maps with random parameters. In Sec. III we discuss the spectrum of generalized dimensions[10–19] and how they can be determined using the Lyapunov number partition function method.[15,18,19] This method is then particularized for maps with uniform Jacobian, and its numerical implementation is discussed. In Sec. IV we use the Lyapunov method to analytically calculate the dimension spectra for the generalized baker's map with random parameters. These results are then compared with those obtained from a numerical implementation of the Lyapunov method, thus providing a test of this implementation and its numerical accuracy. In Sec. V we describe numerical results obtained for the generalized dimensions of the random Hénon map using the Lyapunov method. Finally in Sec. VI we summarize the main conclusions of this paper.

II. SNAPSHOT ATTRACTORS OF RANDOM MAPS

In this section we discuss the qualitative aspects of the attractors of random maps. In order to obtain plots of these attractors we proceed in the following way: take a number of initial conditions N in the basin of attraction of the attractor, iterate each of them n times, and plot the last iterate of all of them. This procedure corresponds to problem 1 of the Introduction, and we refer to it as the snapshot technique. To contrast with this technique, we also take a single initial condition and plot the iterates under the random map. This corresponds to problem 2.

As our first example we consider the well-known Hénon map[20] with random parameters

$$\begin{aligned} x_{i+1}&=a_i-x_i^2+b_iy_i\ ,\\ y_{i+1}&=x_i\ , \end{aligned} \tag{2}$$

where

$$\begin{aligned} a_i&=\bar{a}+\Delta_a r_i\ ,\\ b_i&=\bar{b}+\Delta_b r_i\ , \end{aligned}$$

$\bar{a}$, Δ_a, $\bar{b}$, and Δ_b are fixed parameters, and r_i is a discrete uncorrelated random variable with a uniform probability distribution in the interval $[-1,1]$. We shall always take $\Delta_a\Delta_b=0$, so that at least one of the quantities a or b is nonrandom.

In Fig. 1 we have plotted the snapshot attractor using $N=10^4$ initial conditions in the case of fixed parameters, $\Delta_a=\Delta_b=0$. We see that the attractor is apparently the

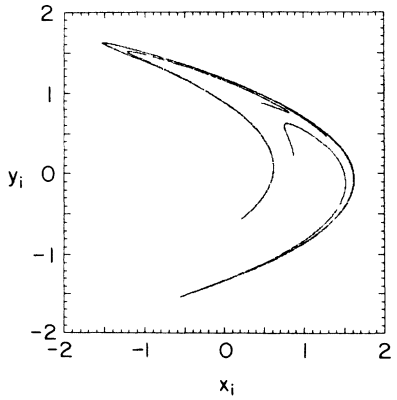

FIG. 1. Attractor of the Hénon map for $\bar{a}=1.15$, $\bar{b}=0.4$, $\Delta_a=\Delta_b=0.0$, $n=250$, $N=10^4$. N is the number of initial conditions; n is the number of iterations.

same as the usual Hénon attractor (see Ref. 20), obtained by iterating a single initial condition and plotting all the iterates (after discarding the initial transient) as it should be.

Turning our attention to the random case we first take $\Delta_a=0$ and $\Delta_b\neq 0$. In Fig. 2 we have plotted all the iterates of a single initial condition; the picture clearly exhibits a smooth density as expected for problem 2. In Fig. 3(a) we have plotted the nth iterate of $N=10^4$ initial conditions for the same parameters as Fig. 2; the resulting snapshot attractor resembles that of a fixed parameter map. In particular, it is fractal. Thus, if we look more closely at the attractor we can recognize the Cantor-set-like structure transverse to the predominantly linear structure. This can be seen in Figs. 3(b) and 3(c) which are enlargements of the small boxes in Figs. 3(a) and 3(b), respectively.

Qualitatively similar results are obtained by taking $\Delta_a\neq 0$ and $\Delta_b=0$. This is illustrated in Fig. 4 where the snapshot attractor of the random map again resembles that of the attractor of the fixed parameter map.

As a second example we consider the so-called Ikeda map[21–23] which models the propagation of a laser field in a ring cavity (a brief description can be found in Grebogi *et al.*[24]). The map has the form

$$\begin{aligned} x_{i+1}&=a+b\,[x_i\cos(\theta_i)-y_i\sin(\theta_i)]\ ,\\ y_{i+1}&=b\,[x_i\sin(\theta_i)+y_i\cos(\theta_i)]\ , \end{aligned} \tag{3}$$

with

$$\theta_i=k-\frac{p_i}{1+x_i^2+y_i^2}\ ,$$

where a, b, and k are fixed parameters and p_i is the random parameter,

$$p_i=\bar{p}+\Delta_p r_i\ ,$$

with r_i as in the case of the Hénon map.

In Figs. 5–7 we have plotted attractors for the Ikeda map for the nonrandom case ($\Delta_p=0$, Fig. 5), for a case corresponding to problem 2 with $\Delta_p=0.5$ (the fuzzy attractor of Fig. 6), and a snapshot attractor with $\Delta_p=0.5$ (Fig. 7). These figures show the same features already found for the Hénon map.

The results presented here for the Hénon and Ikeda maps are typical of two-dimensional maps with random parameters.

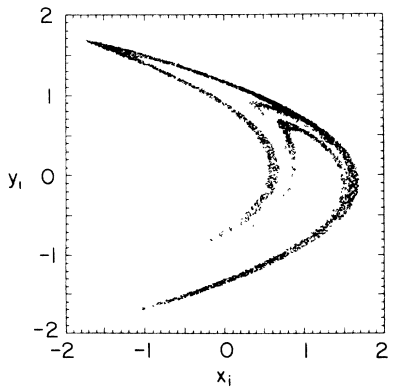

FIG. 2. Attractor of the (random) Hénon map for $\bar{a}=1.15$, $\Delta_a=0.0$, $\bar{b}=0.4$, $\Delta_b=0.05$, $n=10^4$, $N=1$.

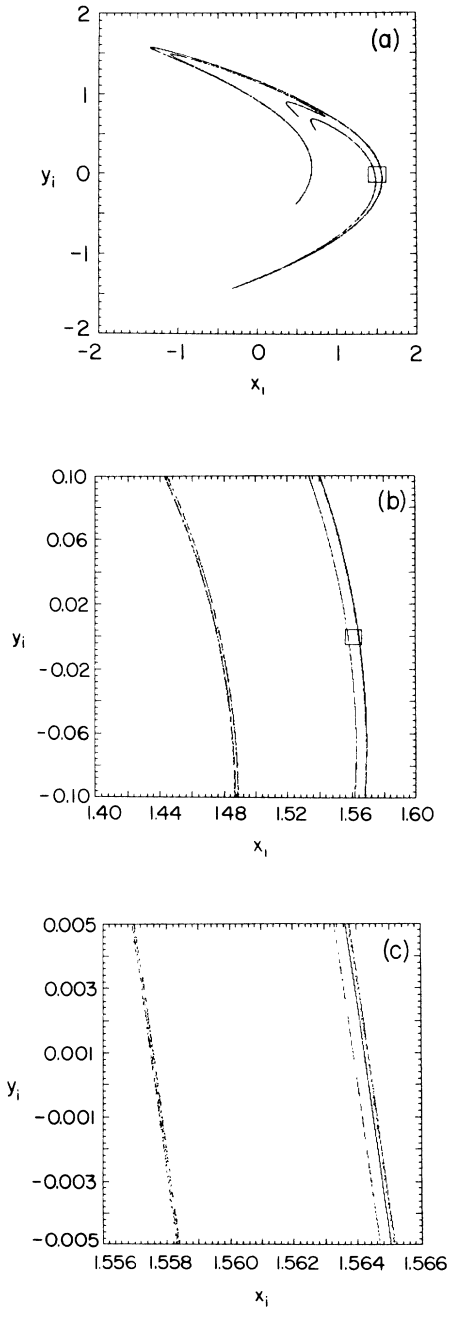

FIG. 3. Attractor of the (random) Hénon map for $\bar{a}=1.15$, $\Delta_a=0.0$, $\bar{b}=0.4$, $\Delta_b=0.05$, $n=250$, and (a) $N=10^4$, (b) $N=2\times 10^5$ [enlargement of the box in (a)], (c) $N=4\times 10^6$ [enlargement of the box in (b)].

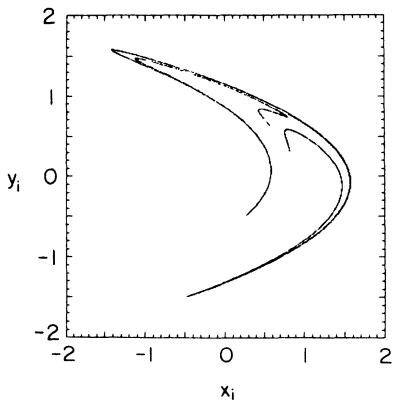

FIG. 4. Attractor of the (random) Hénon map for $\bar{b}=0.4$, $\Delta_b=0.0$, $\bar{a}=1.15$, $\Delta_a=0.05$, $n=250$, $N=10^4$.

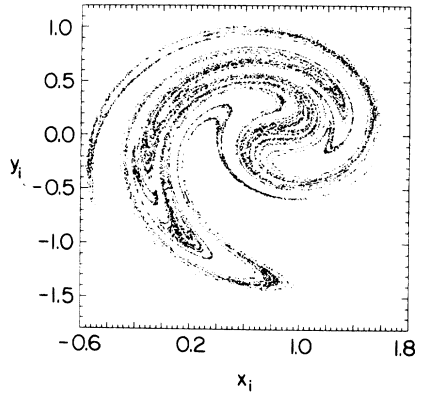

FIG. 5. Attractor of the Ikeda map for $a=0.85$, $b=0.9$, $k=0.4$, $\bar{p}=8.0$, $\Delta_p=0.0$, $n=250$, $N=2\times10^4$.

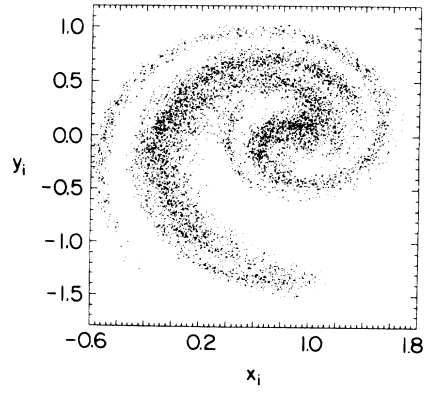

FIG. 6. Attractor of the (random) Ikeda map for $a=0.85$, $b=0.9$, $k=0.4$, $\bar{p}=8.0$, $\Delta_p=0.5$, $n=2\times10^4$, $N=1$.

III. GENERALIZED DIMENSIONS

A. Review of dimension spectra formulations

An important way of quantitatively characterizing the properties of chaotic attractors is through the spectrum of generalized Renyi dimensions commonly denoted by D_q, where q is a real parameter.[10–12] The Renyi dimensions are defined by

$$D_q^{(1)}=\frac{1}{q-1}\lim_{\epsilon\to 0}\frac{\ln\sum_{i=1}^{N(\epsilon)}\pi_i^q}{\ln\epsilon}\ , \tag{4}$$

where π_i is the measure of the attractor in the cube S_i of a grid $\{S_i\}$ of $N(\epsilon)$ cubes of grid size ϵ which cover the phase space. For $q=0$ Eq. (4) reduces to the so-called capacity dimension and in the limit $q\to 1$ to the information dimension (e.g., see Ref. 25).

A more general spectrum of dimensions was introduced by Grassberger[13] and Halsey *et al.*[14] Essentially it generalized $D_q^{(1)}$ in the same way as the Hausdorff dimension[25] generalizes the capacity dimension, by allowing a cover of the measure by a set of cubes $\{S_i\}$ of variable edge lengths ϵ_i. To define this new spectrum, which we denote by $D_q^{(2)}$, one proceeds as follows.

(i) Introduce a quantity

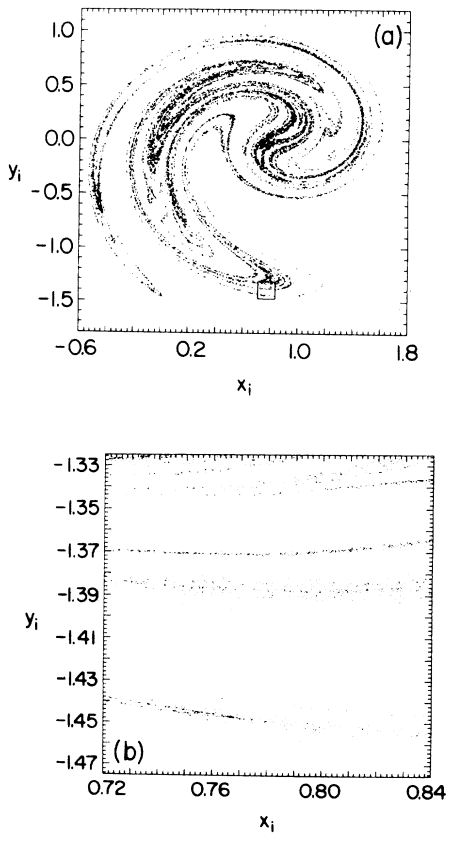

FIG. 7. Attractor of the (random) Ikeda map for $a=0.85$, $b=0.9$, $k=0.4$, $\bar{p}=8.0$, $\Delta_p=0.5$, $n=250$, and (a) $N=2\times10^4$, (b) $N=4\times10^5$ [enlargement of the box in (a)].

$$\Gamma(q,D,\{S_i\},\epsilon)=\sum_i \frac{\pi_i^q}{\epsilon_i^\tau} ,$$

where π_i is the natural measure of the attractor in the cube S_i whose edge length ϵ_i is restricted to be less than ϵ; D is a non-negative parameter and τ is an auxiliary parameter defined by

$$\tau=(q-1)D ;$$

in analogy with statistical mechanics Γ has been called the partition function.

(ii) Optimize over all possible ways of covering the measure to obtain

$$\Gamma^{(2)}(q,D,\epsilon)=\begin{cases}\sup_{\{S_i\}}[\Gamma(q,D,\{S_i\},\epsilon)], & \tau\geq 0\\ \inf_{\{S_i\}}[\Gamma(q,D,\{S_i\},\epsilon)], & \tau\leq 0 .\end{cases}$$

(iii) Take the limit $\epsilon\rightarrow 0$ to obtain

$$\Gamma^{(2)}(q,D)=\lim_{\epsilon\rightarrow 0}\Gamma^{(2)}(q,D,\epsilon) .$$

(iv) Define the generalized dimension as the critical value of D, $D_q^{(2)}$, for which $\Gamma^{(2)}(q,D)$ goes from zero to infinity, that is,

$$\Gamma^{(2)}(q,D)=\begin{cases}0, & \tau<\tau_q^{(2)}\\ \infty, & \tau>\tau_q^{(2)}\end{cases} \tag{5}$$

with

$$\tau_q^{(2)}=(q-1)D_q^{(2)} .$$

These two formulations of the spectrum of generalized dimensions [Eqs. (4) and (5)] are expressed in terms of the natural measure of the attractor. More recently two alternative formulations were introduced which give the spectrum in terms of the dynamical properties of the system, as determined by eigenvalues of the orbits. The first of these, introduced by Morita *et al.*[15] and Grebogi *et al.*,[16,17] gives D_q for nonrandom two-dimensional maps in terms of the eigenvalues of the dense set of periodic saddles on the attractor. A new partition function is defined by (we restrict the definition to the two-dimensional case; for higher-dimensional cases see Grebogi *et al.*[17])

$$\Gamma^{(3)}(q,D,n)=\sum_j(\lambda_{1n}^{(j)})^{-q}(\lambda_{2n}^{(j)})^{-(q-1)(D-1)} , \tag{6a}$$

where $\lambda_{1n}^{(j)}>1>\lambda_{2n}^{(j)}$ are the magnitudes of the unstable and stable eigenvalues of the Jacobian matrix of the n-times-iterated map (that determines the dynamical system) calculated at the jth fixed point of the map and the sum is over all fixed points. Taking the limit $n\rightarrow\infty$ one obtains

$$\Gamma^{(3)}(q,D)=\lim_{n\rightarrow\infty}\Gamma^{(3)}(q,D,n) .$$

The dimension $D_q^{(3)}$ is then determined by Eq. (5) with $\Gamma^{(2)}$ replaced by $\Gamma^{(3)}$ and $\tau_q^{(2)}$ by $\tau_q^{(3)}$.

The second of these dynamical formulations was given by Morita *et al.*,[15] Badii and Politi,[18] and Ott *et al.*[19] A Lyapunov number partition function is defined by

$$\Gamma^{(4)}(q,D,n)=\langle\{\lambda_{1n}(\mathbf{x})[\lambda_{2n}(\mathbf{x})]^{D-1}\}^{1-q}\rangle , \tag{6b}$$

where $\lambda_{1n}>1>\lambda_{2n}$ are the magnitudes of the eigenvalues of the Jacobian matrix of the n-times iterated map for orbits originating at an initial position $\mathbf{x}=(x,y)$ in the basin of attraction, and the angular brackets denote an average with respect to the initial positions $\mathbf{x}$. Taking the limit $n\rightarrow\infty$, we get

$$\Gamma^{(4)}(q,D)=\lim_{n\rightarrow\infty}\Gamma^{(4)}(q,D,n) ,$$

the generalized dimension $D_q^{(4)}$ is again determined by Eq. (5) with $\Gamma^{(2)}$ replaced by $\Gamma^{(4)}$ and $\tau_q^{(2)}$ by $\tau_q^{(4)}$.

The discussions of the periodic points partition function $\Gamma^{(3)}$ (Refs. 15–17) and the Lyapunov number partition function $\Gamma^{(4)}$ (Refs. 15, 18, and 19) were in the context of nonrandom maps. For snapshot attractors of random maps, examination of the original derivations of Eqs. (6) for $\Gamma^{(3)}$ and $\Gamma^{(4)}$ indicates that they still apply. [For the random case, periodic orbits do not exist, but the definition of $\Gamma^{(3)}$ in terms of fixed points of the n-times iterated random map (6a) for a given realization of the random process is still sensible.] In the remainder of this paper we will not consider $\Gamma^{(3)}$ further, but will restrict attention to $\Gamma^{(4)}$ since it appears to offer a much more easily implementable and efficient numerical realization.

How are the different $D_q^{(i)}$ for $i=1,2,3,4$ related to each other? Firstly it can be easily shown that

$$D_q^{(2)}\leq D_q^{(1)} .$$

Furthermore, results obtained in cases where both of these dimensions can be explicitly calculated analytically support the conjecture[14] that they are equal for typical chaotic attractors. It has also been shown[17] that

$$D_q^{(2)}\leq D_q^{(3)} ,$$

and conjectured[19] that the equality holds for typical chaotic attractors below a critical value of q, $q\leq q_T$, where a "phase transition" occurs at q_T.[26–34] Finally it has been conjectured[19,30] that

$$D_q^{(4)}=D_q^{(2)} ,$$

for hyperbolic attractors and also for typical nonhyperbolic attractors provided that q is less than q_T. In addition, for the case $q=1$ (the information dimension), $D_q^{(4)}=D_q^{(2)}$ has been rigorously proven for snapshot attractors of general random maps.[3]

An alternative characterization of natural measures on chaotic attractors was introduced by Halsey *et al.*[14] They consider a spectrum of singularities determined by two indices: a scaling index α, which determines the strength of the singularities, and f_α, which determines how densely the singularities are distributed. These authors show that α and f_α can be obtained from the spectrum D_q by the Legendre transformation

$$\alpha=\frac{d}{dq}[(q-1)D_q] , \tag{7a}$$

$$f_\alpha = q\alpha - (q-1)D_q \ . \tag{7b}$$

In Ref. 14, f_α is interpreted as the Hausdorff dimension of the set of points whose pointwise dimension is α. Actually this statement should be qualified somewhat; f_α appears to be the dimension of the points whose pointwise dimension is α only for hyperbolic attractors or for nonhyperbolic attractors below the phase transition point,[19,30] $q < q_T$.

B. The Lyapunov method: Critical condition

As we have just seen the generalized dimension D_q is the value for D for which $\lim_{n\to\infty}\Gamma(q,D,n)$ goes from 0 to ∞, where Γ is the Lyapunov number partition function defined by Eq. (6b) [from now on we drop the suffix (4) used in Sec. III A]. If we now write Γ in the form

$$\Gamma(q,D,n) = \exp(n l_n) \ ,$$

where l_n is defined by

$$l_n = \frac{1}{n}\ln\Gamma(q,D,n) \ ;$$

the critical condition is equivalent to requiring that $\lim_{n\to\infty} l_n = 0$, that is,

$$\lim_{n\to\infty}\frac{1}{n}\ln\Gamma(q,D_q,n) = 0 \ , \tag{8}$$

provided this limit exists.

For a given realization of the random process, we can use (8) to calculate D_q. For an ensemble of realizations, the D_q for individual realizations are the same with probability one.[7] Denoting this common value of D_q by $\bar{D}_q$, in the case of a random map, l_n will be a random variable with an average value $\bar{l}$, independent of n, and some fluctuation[7] which goes to zero as n goes to ∞. Then the critical condition determining $\bar{D}_q$ takes the form[7]

$$\lim_{n\to\infty}\frac{1}{n}\overline{\ln\Gamma(q,\bar{D}_q,n)} = 0 \ , \tag{9}$$

where the overbar denotes an ensemble average.

C. The Lyapunov method: Maps with uniform Jacobian

The determination of the spectrum of generalized dimensions from the Lyapunov number partition function becomes particularly simple in the case in which the Jacobian determinant of the random map, $J(i)$, is independent of position at each iterate i. Thus the Jacobian determinant of the n-times-iterated random map, J_n, is given by

$$J_n = \prod_{i=1}^{n} J(i) = \lambda_{1n}\lambda_{2n} \ ,$$

and we can use this equation to eliminate λ_{2n} from Eq. (6b) to obtain

$$\Gamma(q,D,n) = J_n^{\eta}\langle\lambda_{1n}^{-\xi}\rangle \ , \tag{10}$$

where the quantities η and ξ are defined by

$$\eta = (q-1)(1-D) \ , \tag{11a}$$

$$\xi = (q-1)(2-D) \ . \tag{11b}$$

Substituting this partition function into the critical condition (8) we obtain an equation giving η in terms of the parameter ξ,

$$\eta_\xi = K_J \lim_{n\to\infty} L_n(\xi) \ , \tag{12}$$

where

$$L_n(\xi) = \frac{1}{n}\ln\langle\lambda_{1n}^{-\xi}\rangle \ , \tag{13}$$

and

$$\frac{1}{K_J} = -\lim_{n\to\infty}\frac{1}{n}\ln J_n \ . \tag{14}$$

Finally the spectrum D_q as a function of q can be obtained in parametric form with parameter ξ from Eqs. (11),

$$q = 1 + \xi - \eta_\xi \ , \tag{15}$$

$$D_q = 1 + \frac{1}{1-\xi/\eta_\xi} \ . \tag{16}$$

The spectrum f_α can also be expressed easily in terms of ξ. Using Eqs. (7) we obtain, after some trivial manipulation,

$$\alpha = 1 + \frac{1}{1-1/\eta'_\xi} \ , \tag{17}$$

$$f_\alpha = 1 + \eta_\xi + \frac{1+\xi-\eta_\xi}{1-1/\eta'_\xi} \ . \tag{18}$$

The quantity $\eta'_\xi \equiv d\eta_\xi/d\xi$ that occurs in these equations can be calculated from Eqs. (12) and (13):

$$\eta'_\xi = K_J \lim_{n\to\infty} L'_n(\xi) \ , \tag{19}$$

where

$$L'_n(\xi) = -\frac{1}{n}\frac{\langle\lambda_{1n}^{-\xi}\ln\lambda_{1n}\rangle}{\langle\lambda_{1n}^{-\xi}\rangle} \ . \tag{20}$$

These results have a simplified form in the cases $q = 0$ (the Hausdorff dimension) and $q \to 1$ (the information dimension), which we record here for later use. For $q = 0$,

$$\begin{aligned} D_0 &= 2 + \xi_0 = f_{\alpha_0} \ , \\ \alpha_0 &= 1 + \frac{1}{1-1/\eta'_{\xi_0}} \ , \end{aligned} \tag{21}$$

where ξ_0 is the solution of the equation

$$1 + \xi_0 - \eta_{\xi_0} = 0 \ .$$

For $q \to 1$,

$$\begin{aligned} D_1 &= 1 + \frac{1}{1-1/\eta'_0} = \alpha_1 = f_{\alpha_1} \ , \\ 1/\eta'_0 &= 1 + \lim_{n\to\infty}\frac{\langle\ln\lambda_{2n}\rangle}{\langle\ln\lambda_{1n}\rangle} \ , \end{aligned} \tag{22}$$

where we have taken into consideration that the limit $q \to 1$ implies $\xi \to 0$. Equation (22) is the Kaplan-Yorke conjecture.[3]

In the special case of a map with fixed Jacobian determinant we have $J(i) \equiv J$ and $J_n = J^n$; Eq. (14) then becomes

$$\frac{1}{K_J} = -\ln J \ . \tag{23}$$

In the case of a map with a random Jacobian determinant, $\ln J_n$ is the sum of n independent random values,

$$\ln J_n = \sum_{i=1}^{n} \ln J(i) \ .$$

For very large value of n this random variable will have a normal distribution and $\ln J_n = n\,\overline{\ln J} + O(n^{1/2})$, where $\overline{\ln J}$ denotes the ensemble average of $\ln J(i)$. Thus Eq. (14) becomes

$$\frac{1}{K_J} = -\overline{\ln J} \ . \tag{24}$$

If j has a probability distribution $\tilde{P}(J)$ and takes values in the interval $\tilde{I}$, then

$$\frac{1}{K_J} = -\int_{\tilde{I}} dJ\, \tilde{P}(J) \ln J \ . \tag{25}$$

D. Numerical implementation of the method and error estimates

The Lyapunov method for the determination of the spectrum of generalized dimensions of a map with uniform Jacobian requires the calculation of the average quantities $\langle \lambda_{1n}^{-\xi} \rangle$ and $\langle \lambda_{1n}^{-\xi} \ln \lambda_{1n} \rangle$. In order to do this we take a large number of initial conditions, N, uniformly distributed in a box placed in the basin of attraction of the attractor, calculate the eigenvalue $\lambda_{1n}^{(i)}$ for each of the corresponding orbits, and substitute in the expressions

$$\langle \lambda_{1n}^{-\xi} \rangle = \frac{1}{N} \sum_{i=1}^{N} (\lambda_{1n}^{(i)})^{-\xi} \ ,$$

$$\langle \lambda_{1n}^{-\xi} \ln \lambda_{1n} \rangle = \frac{1}{N} \sum_{i=1}^{N} (\lambda_{1n}^{(i)})^{-\xi} \ln \lambda_{1n}^{(i)} \ .$$

These two expressions can be written in the form

$$\langle z_n \rangle = \frac{1}{N} \sum_{i=1}^{N} z_n^{(i)} \ ,$$

$$\langle z_n' \rangle = \frac{1}{N} \sum_{i=1}^{N} z_n'^{(i)} \ ,$$

where

$$z_n = \lambda_{1n}^{-\xi} \ ,$$

$$z_n' = -\lambda_{1n}^{-\xi} \ln \lambda_{1n} \ ,$$

and $\{z_n^{(i)}\}_{i=1,N}$, $\{z_n'^{(n)}\}_{i=1,N}$ are the set of values taken by z_n and z_n' for the set of N initial conditions. z_n and z_n' can be considered as random variables and

$$\mu_n = \langle z_n \rangle \ ,$$

$$\mu_n' = \langle z_n' \rangle \ ,$$

are their average values. But μ_n and μ_n' are themselves random variables (the "sample mean"), corresponding to different realizations of the set of N randomly chosen initial conditions. Following Ref. 19, by an argument described in the Appendix, approximations to the standard deviations of these random variables σ_n and σ_n' are given by

$$\sigma_n = \frac{1}{\sqrt{N}} (\langle z_n^2 \rangle - \langle z_n \rangle^2)^{1/2}$$

$$\sigma_n' = \frac{1}{\sqrt{N}} (\langle z_n'^2 \rangle - \langle z_n' \rangle^2)^{1/2} \ ,$$

where

$$\langle z_n^2 \rangle = \frac{1}{N} \sum_{i=N}^{N} (z_n^{(i)})^2 \ ,$$

$$\langle z_n'^2 \rangle = \frac{1}{n} \sum_{i=1}^{N} (z_n'^{(i)})^2 \ .$$

We will use the quantities σ_n and σ_n' as estimates for the errors made in the calculation of the averages $\langle \lambda_{1n}^{-\xi} \rangle$ and $\langle \lambda_{1n}^{-\xi} \ln \lambda_{1n} \rangle$.

The quantities that actually appear in the calculation of the spectra D_q and f_α are not these two averages but the functions of these two averages L_n and L_n' defined by Eqs. (13) and (20). We conclude this section by defining relative errors in these two quantities expressed in terms of μ_n, σ_n, μ_n', and σ_n': (i)

$$E_\sigma(L_n) = \begin{cases} \hat{E}(L_n^{(+)}), & \text{if } |\hat{E}(L_n^{(+)})| \geq |\hat{E}(L_n^{(-)})| \\ \hat{E}(L_n^{(-)}), & \text{otherwise} \end{cases} \tag{26}$$

where

$$\hat{E}(L_n^{(\pm)}) = \frac{L_n^{(\pm)}}{L_n} - 1 \ ,$$

and

$$L_n = \frac{1}{n} \ln \mu_n \ ,$$

$$L_n^{(\pm)} = \frac{1}{n} \ln(\mu_n \pm \sigma_n) \ ; \tag{27}$$

(ii)

$$E_\sigma(L_n') = \begin{cases} \hat{E}(L_n'^{(+)}), & \text{if } |\hat{E}(L_n'^{(+)})| \geq |\hat{E}(L_n'^{(-)})| \\ \hat{E}(L_n'^{(-)}), & \text{otherwise} \end{cases} \tag{28}$$

where

$$\hat{E}(L_n'^{(\pm)}) = \frac{L_n'^{(\pm)}}{L_n'} - 1 \ ,$$

and

$$L_n' = \frac{1}{n} \frac{\mu_n'}{\mu_n} \ ,$$

$$L_n'^{(\pm)} = \frac{1}{n} \frac{\mu_n' \pm \sigma_n'}{\mu_n \mp \sigma_n \operatorname{sgn}(\mu_n' \pm \sigma_n')} \ . \tag{29}$$

IV. THE GENERALIZED BAKER'S MAP

A. Random baker's map and its Lyapunov partition function

The generalized baker's map was introduced in Ref. 25 as a model of dimension studies which is accessible to analysis yet also has nonconstant stretching and contraction. It is a map of the unit square $[0,1]\times[0,1]$ into itself defined by the equations

$$x_{i+1}=ax_i u(c-y_i)+(bx_i+\tfrac{1}{2})u(y_i-c)\ , \tag{30a}$$

$$y_{i+1}=\frac{1}{c}y_i u(c-y_i)+\frac{1}{1-c}(y_i-c)u(y_i-c)\ , \tag{30b}$$

where u is the unit step function,

$$u(\theta)=\begin{cases}0, & \theta<0\\ 1, & \theta>0\end{cases}$$

and the parameters a, b, and c, satisfy the inequalities

$$0<c<1\ ,$$

$$0<a,b\le\tfrac{1}{2}\ .$$

The action of the map on the unit square can be described in the following way (see Fig. 8): divide the square into a bottom part, $[0,1]\times[0,c)$, and a top part $[0,1]\times(c,1]$; compress the bottom (top, respectively) part by a factor a (b, respectively) along the x axis, and stretch it along the y axis by a factor $1/c$ $[1/(1-c)$, respectively], thus obtaining two rectangles, both of vertical height unity, and widths a and b, respectively; move the rectangle of width b so that its lower left corner is at the point $x=\frac{1}{2}$, $y=0$.

In this section we consider a modification of the generalized baker's map in which on each iterate we choose the parameters a, b, and c at random. Let a_i, b_i, and c_i denote the parameter set at iterate i. Consider an orbit, and let $\sigma_i=0$ if $y_i<c_i$ and $\sigma_i=1$ if $y_i>c_i$ [i.e., $\sigma_i=u(y_i-c_i)$]. Also let $\gamma_i=1-\sigma_i$. In terms of these quantities we can express the Jacobian matrix of the random baker's map evaluated at a point $\mathbf{x}_i=(x_i,y_i)$ at iterate i as

$$J(\mathbf{x}_i)=\begin{bmatrix}a_i & 0\\ 0 & 1/c_i\end{bmatrix}\gamma_i+\begin{bmatrix}b_i & 0\\ 0 & 1/(1-c_i)\end{bmatrix}\sigma_i\ .$$

The eigenvalues of this matrix are then

$$\lambda_1(\mathbf{x}_i)=\frac{\gamma_i}{c_i}+\frac{\sigma_i}{1-c_i}\ ,$$

$$\lambda_2(\mathbf{x}_i)=\gamma_i a_i+\sigma_i b_i\ ,$$

and the Jacobian determinant is

$$J(\mathbf{x}_i)=\lambda_1(\mathbf{x}_i)\lambda_2(\mathbf{x}_i)=\gamma_i\frac{a_i}{c_i}+\sigma_i\frac{b_i}{1-c_i}\ .$$

Furthermore, since the Jacobian matrix is diagonal, we can simply express the eigenvalues of the n-times composed random map,

$$\lambda_{1n}=\prod_{i=1}^{n}c_i^{-\gamma_i}(1-c_i)^{-\sigma_i}\ ,$$

$$\lambda_{2n}=\prod_{i=1}^{n}a_i^{\gamma_i}b_i^{\sigma_i}\ . \tag{31}$$

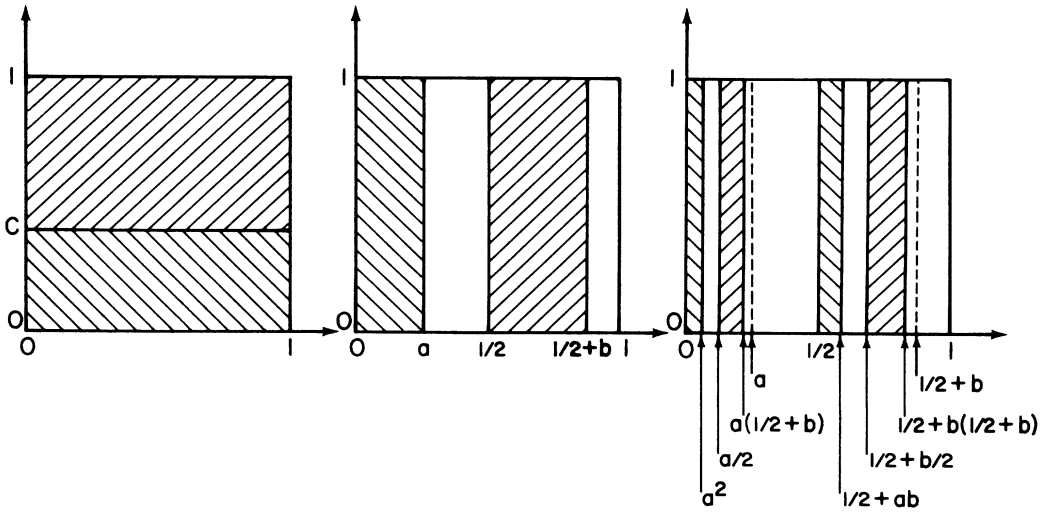

FIG. 8. Generalized baker's map: illustration of two successive applications to the unit square.

From the form of the map the natural measure is uniform along the y direction. Thus, if y_1 is chosen at random with respect to the natural measure [i.e., y_1 is chosen with uniform probability in (0,1)], the probability of the orbit following a given sequence $S_n=\{\sigma_1,\sigma_2,\sigma_3,\ldots,\sigma_n\}$ is

$$\prod_{i=1}^{n} c_i^{\gamma_i}(1-c_i)^{\sigma_i} .$$

Thus the Lyapunov partition function is

$$\Gamma(q,D,n)=\sum_{S_n}\left\{c_1^{\gamma_1}(1-c_1)^{\sigma_1}\left[\prod_{i=1}^{n} c_i^{-\gamma_i}(1-c_i)^{-\sigma_i}\left[\prod_{i=1}^{n} a_i^{\gamma_i}b_i^{\sigma_i}\right]^{D-1}\right]^{1-q}\right\},$$

where the sum is over all possible sequences of zeroes and ones of length n. This can be rewritten as

$$\Gamma(q,D,n)=\sum_{S_n}\left[\prod_{i=1}^{n}(c_i^q a_i^\eta)^{\gamma_i}[(1-c_i)^q b_i^\eta]^{\sigma_i}\right],$$

where $\eta=(1-q)(D-1)$, from which we see that the Lyapunov partition function for the random baker's map takes the simple form

$$\Gamma(q,D,n)=\prod_{i=1}^{n}[c_i^q a_i^\eta+(1-c_i)^q b_i^\eta] . \tag{32}$$

B. Calculation of dimension spectra for the random baker's map

Let us assume, for simplicity, that only one of the parameters is allowed to vary randomly. We denote this parameter by p and rewrite Eq. (32) in the form

$$\Gamma(q,D,n)=\prod_{i=1}^{n}\Gamma(q,D;p_i) . \tag{33}$$

Substituting this partition function in the critical condition (8) we obtain

$$\lim_{n\to\infty}\frac{1}{n}\sum_{i=1}^{n}\overline{\ln\Gamma(q,D_q;p_i)}=0 .$$

If we assume that the parameter p follows some probability distribution $\tilde{P}(p)$, and takes values in some interval $\tilde{I}$, then this condition becomes

$$\int_{\tilde{I}} dp\,\tilde{P}(p)\ln\Gamma(q,D_q;p)=0 . \tag{34}$$

This equation can be explicitly solved in two particular cases.

Case I: $a=b$ fixed, c random. $a<c<(1-a)$; this condition is necessary to guarantee that the Jacobian determinant of the generalized baker's map is less than 1. From Eq. (32) and (33) we obtain

$$\Gamma(q,D;c)=a^\eta S(q;c) ,$$

where

$$S(q;c)=c^q+(1-c)^q ,$$

which on substitution in Eq. (34) gives

$$\eta_q=K_a\int_{\tilde{I}} dc\,\tilde{P}(c)\ln S(q;c) ,$$

where

$$K_a=-(\ln a)^{-1} .$$

We now take c to be of the form

$$c=\bar{c}+\Delta_c r ,$$

where $\bar{c}$ and Δ_c are fixed and r is a random variable with uniform probability distribution $P(r)=\frac{1}{2}$ in the interval $I=[-1,1]$. We obtain

$$\eta_q=\frac{K_a}{2\Delta_c}\int_{\bar{c}-\Delta_c}^{\bar{c}+\Delta_c} dc\,\ln S(q;c) . \tag{35}$$

From (11a) the spectrum D_q is given by

$$D_q=1+\frac{\eta_q}{1-q} . \tag{36}$$

As regards the spectrum f_α, Eqs. (7) yields

$$\alpha=1-\eta_q' , \tag{37}$$

$$f_\alpha=1+\eta_q-q\eta_q' , \tag{38}$$

where $\eta_q'\equiv d\eta_q/dq$ which from (35) is

$$\eta_q'=\frac{K_a}{2\Delta_c}\int_{\bar{c}-\Delta_c}^{\bar{c}+\Delta_c} dc\,\frac{S'(q;c)}{S(q;c)} , \tag{39}$$

with $S'\equiv dS/dq$.

The two integrals that occur in Eqs. (35) and (39) cannot in general be calculated analytically. The two exceptions are for $q=0$ and $q\to 1$, for which one obtains

$$\eta_0=K_a\log_{10}2 ,$$

$$\eta_0'=\frac{K_a}{4\Delta_c}\tilde{G}_0(\bar{c},\Delta_c) ,$$

$$\eta_1=0 ,$$

$$\eta_1'=\frac{K_a}{2\Delta_c}\tilde{G}_1(\bar{c},\Delta_c) ,$$

where

$$\tilde{G}_i(\bar{c},\Delta_c)=G_i(c_+)-G_i(c_-)+G_i(1-c_-)-G_i(1-c_+) ,$$

for $i=0,1$, $c_\pm=\bar{c}\pm\Delta_c$, and

$$G_0(\theta)=\theta(\ln\theta-1) ,$$

$$G_1(\theta)=\frac{\theta_2}{4}(2\ln\theta-1) . \tag{40}$$

From these results one obtains

$$D_0=1+\eta_0=f_{\alpha_0} ,$$

$$\alpha_0=1-\eta_0' ,$$

$$D_1=1-\eta_1'=\alpha_1=f_{\alpha_1} .$$

Note that the Hausdorff dimension, $D_0=1+K_a\ln 2$, is independent of c.

The spectrum D_q is a decreasing function of q with asymptotic values at $q\to\pm\infty$ given by

$$D_{-\infty}=1-\frac{K_a}{2\Delta_c}\times\begin{cases}G_0(c_+)-G_0(c_-), & \text{if } c_+<\frac{1}{2}\\ 2G_0(\frac{1}{2})-G_0(c_-)-G_0(1-c_+), & \text{if } c_+>\frac{1}{2}\end{cases}$$

$$D_{+\infty}=1-\frac{K_a}{2\Delta_c}\times\begin{cases}G_0(1-c_-)-G_0(1-c_+), & \text{if } c_+<\frac{1}{2}\\ G_0(1-c_-)+G_0(c_+)-2G_0(\frac{1}{2}), & \text{if } c_+>\frac{1}{2}\end{cases}$$

The spectrum f_α has a bell shape with a maximum value D_0 occurring at $\alpha=\alpha_0$. α_0 is precisely the arithmetic mean of the two values of α for which $f_\alpha=1$,

$$\alpha_0=\tfrac{1}{2}(\alpha_{-\infty}+\alpha_{+\infty}) ,$$

where $\alpha_{\mp\infty}=D_{\mp\infty}$.

These results for the dimension spectra are illustrated in Figs. 9 and 10. In Fig. 9, which corresponds to the nonrandom case (recovered by taking the limit $\Delta_c\to 0$), we have plotted the spectra D_q and f_α for different values of $\bar{c}$ (with a kept fixed). In Fig. 10 we have plotted the spectra D_q and f_α for $\bar{c}=\frac{1}{2}$ and different values of Δ_c (with a kept fixed).

Case II: $a/c=b/(1-c)=J, c$ fixed, J random. From Eqs. (32) and (33) we obtain

$$\Gamma(q,D;J)=J^\eta S(1+\xi;c) ,$$

which on substitution into Eq. (34) gives

$$\eta_\xi=K_J\ln S(1+\xi;c) ,$$

where K_j is now defined by

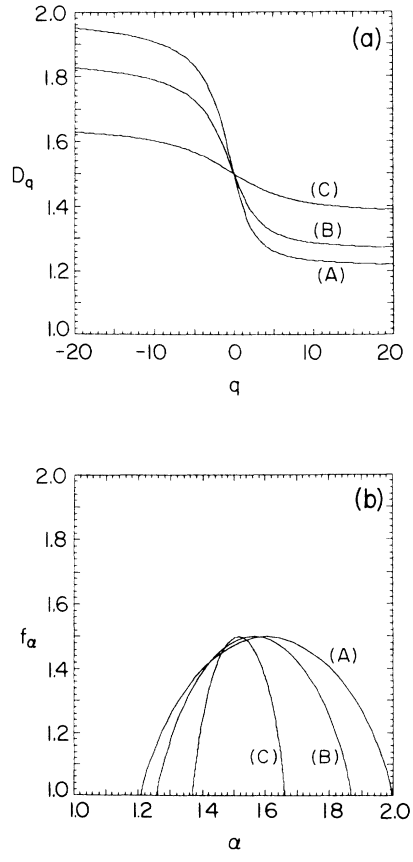

FIG. 9. Baker's map (case I—exact results): spectra of generalized dimensions and scaling indices, (a) D_q vs q, (b) f_α vs α for $a=b=0.25$, $\Delta_c=0.0$, $\bar{c}=0.251$ [curve (*A*)], 0.3 [curve (*B*)], 0.4 [curve (*C*)].

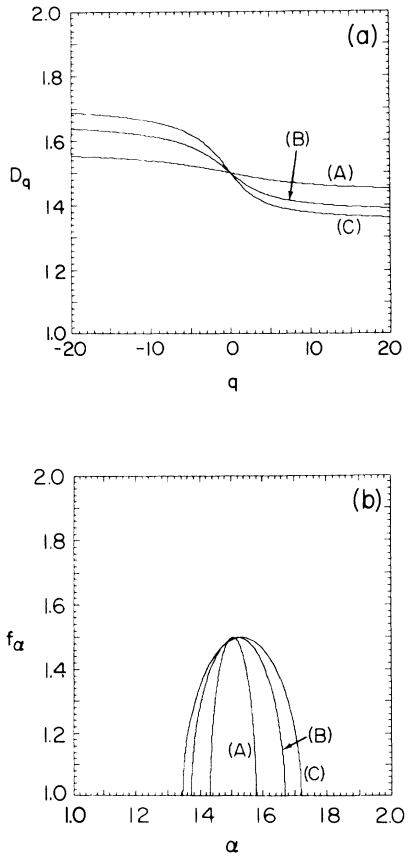

FIG. 10. Random baker's map (case I—exact results): spectra of generalized dimensions and scaling indices (a), D_q vs q, (b) f_α vs α, for $a=b=0.25$, $\bar{c}=0.5$, $\Delta_c=0.1$ [curve (*A*)], 0.2 [curve (*B*)], 0.249 [curve (*C*)].

$$\frac{1}{K_J} = -\int_{\bar{I}} dJ\, \tilde{P}(J) \ln J \ .$$

Note that this parametric formulation in terms of the quantity ξ coincides with that introduced more generally in Sec. III. Consequently the quantities q, D_q, α, and f_α can be obtained using Eqs. (15)–(18). In the particular cases $q=0$ and $q \to 1$ Eqs. (21) and (22) apply.

The asymptotic values of D_q at $q \to \mp \infty$ take simple forms:

$$D_{\mp\infty} = 1 + \frac{1}{1 - 1/\eta'_{\mp\infty}} \ ,$$

where

$$\eta'_{-\infty} = K_J \ln c \ ,$$

$$\eta'_{+\infty} = K_J \ln(1-c) \ .$$

If we now take J to be of the form

$$J = \bar{J} + \Delta_J r \ ,$$

where $\bar{J}$ and Δ_J are fixed and r is a random variable with uniform probability distribution in the interval $[-1,1]$, then

$$\frac{1}{K_J} = -\frac{1}{2\Delta_J}[G_0(\bar{J}+\Delta_J) - G_0(\bar{J}-\Delta_J)] \ ,$$

where G_0 was defined in Eq. (40). The nonrandom case can be recovered by taking the limit $\Delta_J \to 0$:

$$\frac{1}{K_J} = -\ln \bar{J} \ .$$

The results for the dimension spectra are illustrated in Figs. 11 and 12. In Fig. 11, which corresponds to the nonrandom case, we have plotted the spectra D_q and f_α for different values of $\bar{J}$ (with c kept fixed). In Fig. 12 we have plotted the spectra D_q for $\bar{J}$ fixed and different values of Δ_J (with c also kept fixed).

C. Error estimates

The generalized baker's map, in the case of uniform Jacobian (case II), offers the possibility of testing the nu-

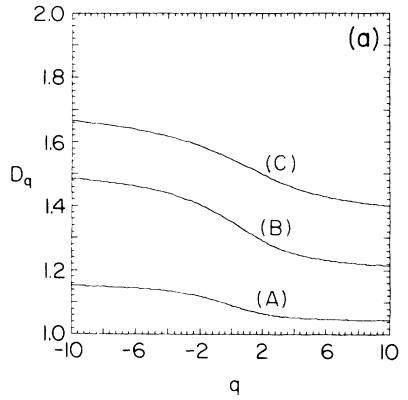

FIG. 11. Baker's map (case II—exact results): spectra of generalized dimensions and scaling indices, (a) D_q vs q, (b) f_α vs α, for $c=0.25$, $\Delta_J=0.0$, $\bar{J}=0.001$ [curve (A)], 0.3 [curve (B)], 0.599 [curve (C)].

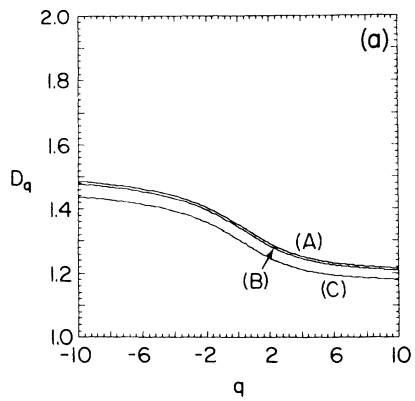

FIG. 12. Random baker's map (case II—exact results): spectra of generalized dimensions and scaling indices, (a) D_q vs q, (b) f_α vs α, for $c=0.25$, $\bar{J}=0.3$, $\Delta_J=0.0$ [curve (A)], 0.15 [curve (B)], 0.299 [curve (C)].

merical procedure for determining the spectrum of generalized dimensions based on the Lyapunov number partition function. In fact, we found in Sec. III that

$$\eta_\xi = K_J \lim_{n\to\infty} L_n(\xi) ,$$

$$\eta'_\xi = K_J \lim_{n\to\infty} L'_n(\xi) ,$$

where L_n and L'_n are defined by Eqs. (13) and (20), while in this section we obtained

$$\eta_\xi = K_J L(\xi) ,$$

$$\eta'_\xi = K_J L'(\xi) ,$$

where

$$L(\xi) = \ln S(1+\xi;c) ,$$

$$L'(\xi) = \frac{S'(1+\xi;c)}{S(1+\xi;c)} .$$

We are therefore led to define the relative error in the quantities L_n and L'_n by

$$E(L_n) = \frac{L_n(\xi)}{L(\xi)} - 1 ,$$

$$E(L'_n) = \frac{L'_n(\xi)}{L(\xi)} - 1 . \tag{41}$$

In Fig. 13 we have plotted the exact errors $E(L_n)$ and $E(L'_n)$ versus ξ for different values of n (the curves are labeled by a number m defined by $m = n/5$). The numerical calculations of L_n and L'_n were done using $N = 10^6$ randomly chosen initial conditions. The figure refers to the baker's map with J fixed; the results for J random are quite similar. These plots show that: (i) the errors are very small for $|\xi| \lesssim 1$ and for all values of m; (ii) in general, the errors increase with $|\xi|$ and with m, more significantly so for negative ξ; (iii) the errors remain very small for all values of ξ for $m = 1$; (iv) in general, $|E(L'_n)|$ is larger than $|E(L_n)|$.

In Fig. 14 we have plotted the statistical errors $E_\sigma(L_n)$ and $E_\sigma(L'_n)$, defined by Eqs. (26) and (28), versus ξ for different values of n. The figure refers to the baker's map with J fixed. $E_\sigma(L_n)$ gives a good qualitative portrait of

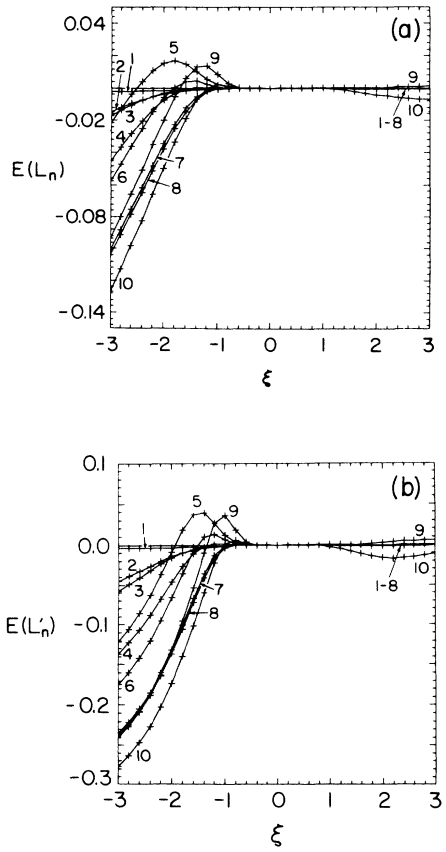

FIG. 13. Baker's map (case II): dependence of the (exact) errors E [defined by Eq. (41)] on ξ and n, (a) $E(L_n)$ vs ξ, (b) $E(L'_n)$ vs ξ, for $c = 0.25$, $\bar{J} = 0.3$, $\Delta_J = 0.0$, $N = 10^6$. The curves are labeled by a number m defined by $m = n/5$.

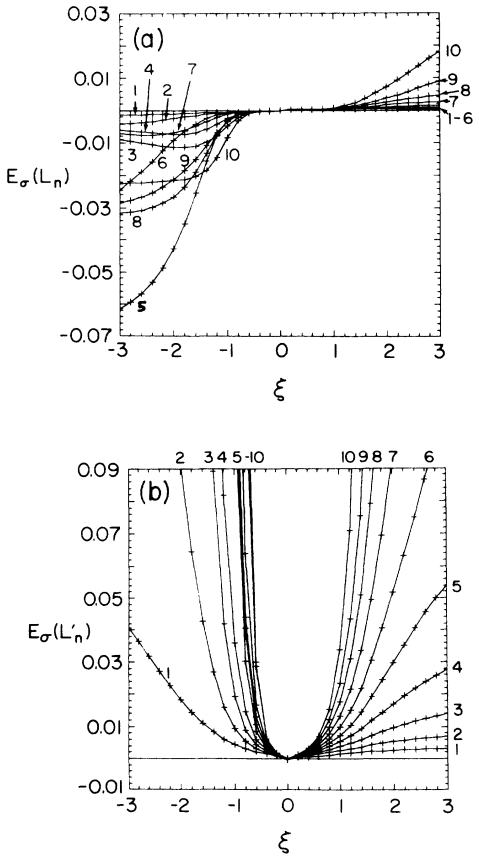

FIG. 14. Baker's map (case II): dependence of the (exact) errors E_σ [defined by Eqs. (26) and (28)] on ξ and n, (a) $E_\sigma(L_n)$ vs ξ, (b) $E_\sigma(L'_n)$ vs ξ, for $c = 0.25$, $\bar{J} = 0.3$, $\Delta_J = 0.0$, $N = 10^6$. The curves are labeled by a number of m defined by $m = n/5$.

the error [cf. Fig. 13(a)]. $E_\sigma(L_n')$ seems to be of more limited use, besides emphasizing that the reliability of the method decreases as $|\xi|$ increases.

Note that, while the error in L_n and L_n' is smallest for small n, we still need large n to obtain an accurate estimate of the dimensions D_q, in conformity with the limit $n \to \infty$ in (8). In practice, however, we expect accurate results for not too large n (i.e., larger than any correlation time of the orbits).

V. THE HÉNON MAP

We now describe the numerical results obtained for the Hénon map defined in Eq. (2). These results can be divided into two groups. In the first group (Figs. 15 and 16) we essentially discuss the errors intrinsic to the method; all these figures refer to the Hénon map with fixed parameters, the results being similar for the random case. In the second group (Figs. 17 and 18) we consider the influence of the randomness on the spectra of generalized dimensions and of scaling indices.

In Fig. 15 we have plotted the quantities L_n and L_n', defined by Eqs. (13) and (20), versus ξ for different values of n. We see that the dependence of L_n and L_n' (especially L_n) on n is slight for values of ξ below some "transition" value ξ_T, roughly around 1. For $\xi \simeq \xi_T$ the quantity L_n' becomes positive and the method breaks down; this is due to the appearance of values of λ_{1n} less than 1, and therefore to homoclinic tangencies. The failure of the method is compatible with the existence of a "phase transition" at $\xi = 1$, as determined by Ott *et al.*[32] and Grassberger *et al.*[30]

In Fig. 16 we have plotted the errors $E_\sigma(L_n)$ and $E_\sigma(L_n')$, defined by Eqs. (26) and (28), versus ξ for different values of n. In these plots we can clearly distinguish two regions, $\xi < \xi_T$ and $\xi \simeq \xi_T$. In the first of these regions we further distinguish two subregions: for values of ξ close to the origin the errors remain very small and practically independent of n; as ξ becomes more negative the errors start increasing and depending on n, although they remain small for at least some of the values of n. In the second region the errors increase very steeply with in-

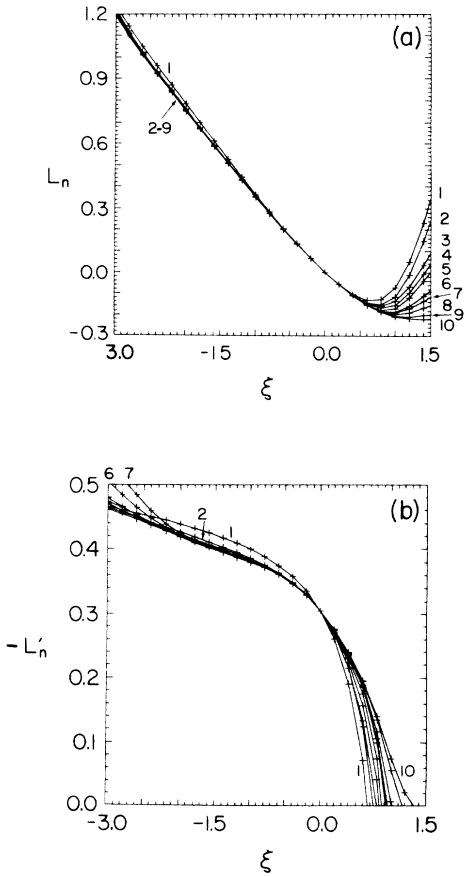

FIG. 15. Hénon map: dependence of the quantities L_n and L_n' on ξ and n, (a) L_n vs ξ, (b) L_n' vs ξ, for $\bar{a} = 1.2$, $\bar{b} = 0.3$, $\Delta_a = \Delta_b = 0.0$, $N = 10^7$. The curves are labeled by a number m defined by $m = n/5$.

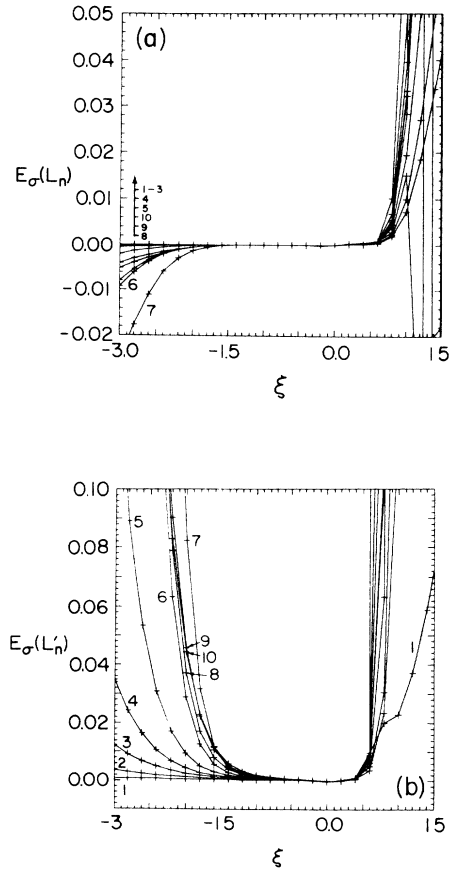

FIG. 16. Hénon map: dependence of the relative errors E_σ on ξ and n, (a) $E_\sigma(L_n)$ vs ξ, (b) $E_\sigma(L_n')$ vs ξ, for $\bar{a} = 1.2$, $\bar{b} = 0.3$, $\Delta_a = \Delta_b = 0.0$, $N = 10^7$. The curves are labeled by a number m defined by $m = n/5$.

creasing ξ for all values of n, indicating the breakdown of the calculation.

In Fig. 17 we have plotted the spectra of generalized dimensions D_q and of scaling indices f_α for the Hénon map in the three cases: Curve (A) $\Delta_a=\Delta_b=0$; curve (B) $\Delta_b\neq 0$, $\Delta_a=0$; curve (C) $\Delta_a\neq 0$, $\Delta_b=0$. Curves (A'), (B') and (C') are copies of curves A, B, and C shifted upward by 0.1, 0,2, and 0.3, respectively. The experimental points on these curves are labeled by the values of the parameter ξ.

In Fig. 18(a) we have plotted the Hausdorff and information dimensions as functions of the randomness parameters Δ_b (with $\Delta_a=0$) and in Fig. 18(b) as a function of Δ_a (with $\Delta_b=0$). The Hausdorff dimension was calculated by using a Newton-Raphson method to determine the parameter ξ_0 that occurs in Eq. (21). Considering the values of the parameter ξ involved in the calculations of D_0 and D_1 ($\simeq -0.8$ and 0, respectively) one expects the accuracy of the method to be high. To emphasize this point and to relate our results to those of other authors we have used our numerical procedure to determine the Hausdorff dimension of the Hénon map with the more usual parameter values, $a=1.4$ annd $b=0.3$: we obtained $D=1.2750\pm\epsilon$, with $\epsilon<10^{-4}$ given by the statistical procedure of Sec. III D; this value is in good agreement with that reported by Badii and Politi.[18]

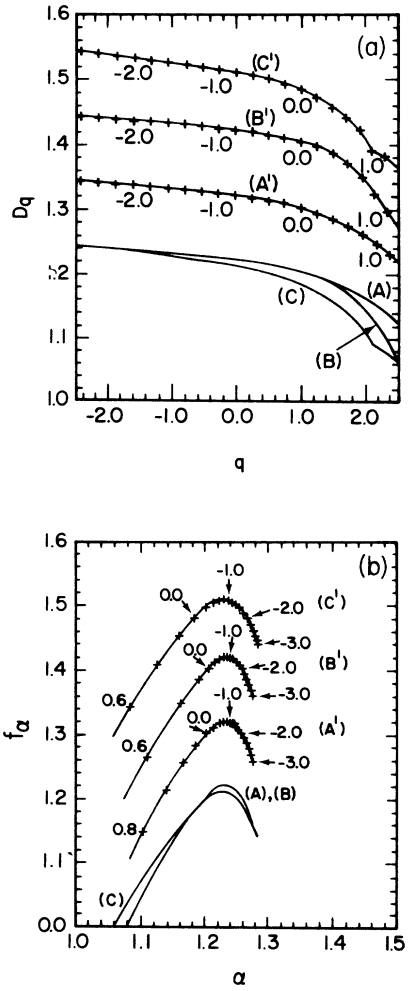

FIG. 17. Hénon map: spectra of generalized dimensions and of scaling indices, (a) D_q vs q, (b) f_α vs α, for $\bar{a}=1.2$, $\bar{b}=0.3$, $n=50$, $N=10^7$; and curve (A), $\Delta_a=0.0$, $\Delta_b=0.0$; curve (B) $\Delta_a=0.0$, $\Delta_b=0.01$; curve (C) $\Delta_a=0.1$, $\Delta_b=0.0$. Curves (A'), (B'), and (C') are copies of curves (A), (B), and (C) shifted upwards by amounts 0.1, 0.2, and 0.3, respectively; on these curves the experimental points (+) are labeled by values of the parameter ξ.

VI. CONCLUSIONS

We have studied qualitative and quantitative properties of attractors of two-dimensional random maps. As regards the qualitative properties, we have used a snapshot technique (in which we plot a certain iterate of a large number of initial conditions in the basin of attraction of the attractor) to obtain pictures of the attractors; these

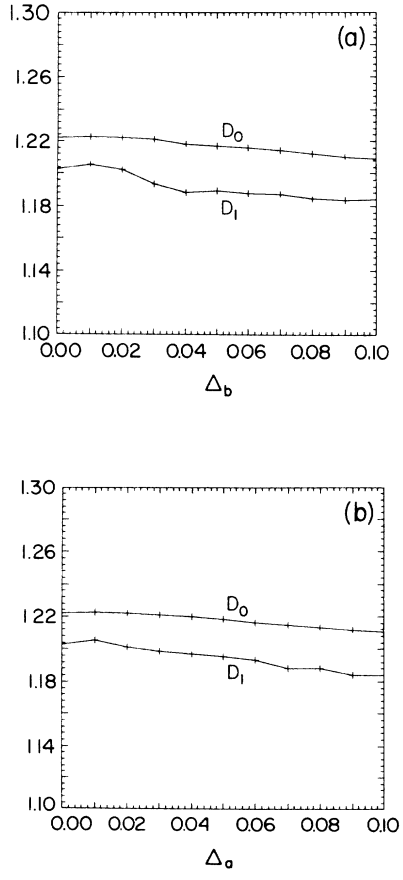

FIG. 18. Hénon map: dependence of the Hausdorff and information dimensions on randomness, (a) D_0,D_1 vs Δ_b, for $\bar{a}=1.2$, $\Delta_a=0.0$, $\bar{b}=0.3$; (b) D_0,D_1 vs Δ_a, for $\bar{a}=1.2$, $\bar{b}=0.3$, $\Delta_b=0.0$.

pictures show similarity with attractors of fixed parameter maps, including a Cantor-set-like transverse structure.

As regards the quantitative properties, we have used the Lyapunov number partition function method to calculate the spectra of generalized dimensions and of scaling indices of these attractors. We first considered the generalized baker's map which is amenable to analytical treatment; we obtained expressions for the spectra and discussed how the randomness affects them; we also examined the errors involved in a numerical implementation of the Lyapunov method. Finally we applied this numerical method to the Hénon map with random parameters; in particular we obtained curves showing how the Hausdorff and information dimensions change with the randomness. Our results indicate that the Lyapunov partition function technique can be implemented for the numerical calculation of dimension spectra for snapshot attractors of random maps, and that the statistical error (i.e., the error due to calculating Γ using a finite number of orbits) in the method can be estimated in a straightforward way.

ACKNOWLEDGMENTS

This work was supported by the U.S. Department of Energy (Office of Basic Energy Sciences—Applied Mathematics Program), the Office of Naval Research (Physics), and the Portuguese Junta Nacional de Investigação Científica e Tecnológica.

APPENDIX

We obtain an estimate for the error made in the calculation of the averages $\langle \lambda_{1n}^{-\xi} \rangle$ and $\langle \lambda_{1n}^{-\xi} \ln \lambda_{1n} \rangle$.

We assume that $z = \lambda_{1n}^{-\xi}$ (or $-\lambda_{1n}^{-\xi} \ln \lambda_{1n}$) is a discrete random variable which takes the set of values $\{z_i\}_{i=1,N}$ for the N initial conditions. From this set of values we can calculate the averages

$$\langle z \rangle = \frac{1}{N} \sum_{i=1}^{N} z_i ,$$

$$\langle z^2 \rangle = \frac{1}{N} \sum_{i=1}^{N} z_i^2 ,$$

and the variance of z,

$$\sigma_z = (\langle z^2 \rangle - \langle z \rangle^2)^{1/2} .$$

But $\langle z \rangle$, the quantity we are really interested in, is itself a random variable which takes different values for different sets of N initial conditions; let μ denote this random variable. We are interested in calculating the standard deviation of μ, defined by

$$\sigma_\mu = (\overline{\mu^2} - \bar{\mu}^2)^{1/2} ,$$

where the overbar here denotes average over all possible sets of N initial conditions. Using the definition of μ we have

$$\begin{aligned} \overline{\mu^2} &= \frac{1}{N^2} \overline{\sum_{i,j=1}^{N} z_i z_j} \\ &= \frac{1}{N^2} \left[\overline{\sum_{i=1}^{N} z_i^2 + \sum_{\substack{i,j=1 \\ i \neq j}}^{N} z_i z_j} \right] \\ &= \frac{1}{N^2} \left[\overline{N \langle z^2 \rangle + \sum_{\substack{i,j=1 \\ i \neq j}}^{N} z_i z_j} \right] . \end{aligned}$$

Approximating each of the z_i's in this last equation by their average value, that is, $z_i \simeq \langle z \rangle$, we obtain

$$\begin{aligned} \overline{\mu^2} &\simeq \frac{1}{N^2} \overline{[N \langle z^2 \rangle + N(N-1) \langle z \rangle^2]} \\ &= \frac{1}{N} \overline{\langle z^2 \rangle} + \left[1 - \frac{1}{N} \right] \overline{\langle z \rangle^2} . \end{aligned}$$

Substituting $\overline{\mu^2}$ and $\bar{\mu} = \overline{\langle z \rangle}$ into the expression of σ_μ and assuming that the values of $\langle z \rangle$ and $\langle z^2 \rangle$ are approximately the same for all sets of initial conditions, we have

$$\sigma_\mu \simeq \frac{1}{\sqrt{N}} \sigma_z .$$

Note that these error estimates are for the errors incurred by using a finite number of orbits N in calculating the averages over position $\langle\ \rangle$ for a given realization of the random process. They do not address the statistical spread in $\langle\ \rangle$ that occurs for different realizations. (This latter spread should decrease with the number of iterates.)

[1]Ya. G. Sinai, Usp. Mat. Nauk. **27** (4), 21 [Russ. Math Surv. **27** (4), 21 (1972)]; R. Bowen and D. Ruelle, Invent. Math. **29**, 181 (1975).

[2]Some examples of work along these lines are the following (see also the references they contain): Iu. I Kifer, Izv. Akad. Nauk. SSSR Ser. Math. Tom **38**, No. 5 (1974) [Math. USSR Izvestija **8**, 1083 (1974)]; R. V. Jensen and C. Oberman, Phys. Rev. Lett. **46**, 1547 (1981); D. Ruelle, Commun. Math. Phys. **82**, 137 (1981); E. Ott, E. Yorke, and J. A. Yorke, Physica **26D**, 62 (1985); E. Ott and J. D. Hanson, Phys. Lett. **85A**, 20 (1981).

[3]An exception is the paper of F. Ledrappier and L.-S. Young [Commun. Math. Phys. **117**, 529 (1988)] which proves that the information dimension of the sample measure resulting from the composition of N-dimensional random diffeomorphisms ($N \geq 2$) is given by the Lyapunov dimension as conjectured by Kaplan and Yorke. (A proof of this for the nonrandom case does not exist except for dimension 2.)

[4]M. R. Maxey and J. J. Riley, Phys. Fluids **26**, 883 (1983).

[5]L. Yu, C. Grebogi, and E. Ott (unpublished).

[6]E. Ott and T. M. Antonsen, Phys. Rev. Lett. **61**, 2839 (1988).

[7]E. Ott and T. M. Antonsen, Phys. Rev. A **39**, 3660 (1989).

[8]B. B. Mandelbrot, J. Fluid Mech. **62**, 331 (1974); K. R. Sreenivasan and C. Meneveau, Phys. Rev. A **38**, 6287 (1988); U. Frisch and G. Parisi, in *Turbulence and Predictability in Geophysical Fluid Dynamics and Climate Dynamics*, edited by

M. Ghil, R. Benzi, and G. Parisi (North-Holland, New York, 1985), p. 84.
[9]Experiments determining the fractal nature of the distribution of the gradient squared of passive scalars in fully developed turbulent flows appear in R. R. Prasad, C. Meneveau, and K. R. Sreenivasan, Phys. Rev. Lett. **61**, 74 (1988).
[10]A. Renyi, *Probability Theory* (North-Holland, Amsterdam, 1970).
[11]P. Grassberger, Phys. Lett. **97A**, 227 (1983).
[12]H. G. E. Hentschel and I. Procaccia, Physica **8D**, 435 (1983).
[13]P. Grassberger, Phys. Lett. **107A**, 101 (1985).
[14]T. C. Halsey, M. H. Jensen, L. P. Kadanoff, I. Procaccia, and B. I. Shraiman, Phys. Rev. A **33**, 1141 (1986).
[15]T. Morita, H. Hata, H. Mori, T. Horita, and K. Tomita, Prog. Theor. Phys. **78**, 511 (1987).
[16]C. Grebogi, E. Ott, and J. A. Yorke, Phys. Rev. A **36**, 3522 (1987).
[17]C. Grebogi, E. Ott, and J. A. Yorke, Phys. Rev. A **37**, 1711 (1988).
[18]R. Badii and A. Politi, Phys. Rev. A **35**, 1288 (1987).
[19]E. Ott, T. Sauer, and J. A. Yorke, Phys. Rev. A **39**, 4212 (1989).
[20]M. Hénon, Commun. Math. Phys. **50**, 69 (1976).
[21]K. Ikeda, Opt. Commun. **30**, 257 (1979).
[22]K. Ikeda, H. Daido, and O. Akimoto, Phys. Rev. Lett. **45**, 709 (1980).
[23]S. M. Hammell, C. K. R. T. Jones, and J. V. Moloney, J. Opt. Soc. Am. B **2**, 552 (1985).
[24]C. Grebogi, E. Ott, F. Romeiras, and J. A. Yorke, Phys. Rev. A **36**, 5365 (1987).
[25]J. D. Farmer, E. Ott, and J. A. Yorke, Physica **7D**, 153 (1983).
[26]P. Cvitanovic, in Proceedings of the Workshop on Condensed Matter, Atomic and Molecular Physics, Trieste, Italy, 1986 (unpublished).
[27]T. Bohr and M. H. Jensen, Phys. Rev. A **36**, 4904 (1987).
[28]D. Katzen and I. Procaccia, Phys. Rev. Lett. **58**, 1169 (1987).
[29]P. Szépfalusy, T. Tél, A. Csordas, and Z. Kovacs, Phys. Rev. A **36**, 3525 (1987).
[30]P. Grassberger, R. Badii, and A. Politi, J. Stat. Phys. **51**, 135 (1988).
[31]M. Kohmoto, Phys. Rev. A **37**, 1345 (1988).
[32]E. Ott, C. Grebogi, and J. A. Yorke, Phys. Lett. **135A**, 343 (1989).
[33]A. Politi, R. Badii, and P. Grassberger, J. Phys. A **21**, L763 (1988).
[34]E. Ott, W. D. Withers, and J. A. Yorke, J. Stat. Phys. **36**, 687 (1984).